Soft Matter

RSC Publishing

PAPER

View Article Online
View Journal | View Issue

Cite this: *Soft Matter*, 2013, **9**, 2308

Experimental determination of bending rigidity and saddle splay modulus in bicontinuous microemulsions

Olaf Holderer,*[a] Henrich Frielinghaus,[a] Michael Monkenbusch,[b] Michael Klostermann,[c] Thomas Sottmann[c] and Dieter Richter[ab]

Received 24th October 2012
Accepted 26th December 2012

DOI: 10.1039/c2sm27449c

www.rsc.org/softmatter

Elastic properties of surfactant membranes can be described in terms of the bending rigidity κ and the saddle splay modulus $\bar{\kappa}$. Phase diagram measurements and neutron scattering experiments allowed the determination of these parameters. Recent simulations showed that the bending rigidity, which is deduced from the characteristic length scales in the microemulsion, is a mixture of $\bar{\kappa}$ and κ. By combining neutron spin echo (NSE) spectroscopy, small angle neutron scattering (SANS) and phase diagram measurements, we show that also experimentally the different contributions can be separated. For supercritical CO_2 microemulsions and bicontinuous microemulsions with additives, the prefactors of the $\bar{\kappa}$ and κ contributions are determined and compared to those from simulations.

1 Introduction

Microemulsions are thermodynamically stable mixtures of oil, water and a surfactant and can self-assemble into a variety of local structures, depending on temperature and composition. Droplets, lamellar, hexagonal, cubic or bicontinuous structures are some examples. In bicontinuous microemulsions, oil and water channels interpenetrate each other in a sponge-like structure, separated from a surfactant layer. They are theoretically often described in terms of the Gaussian random field model (GRFM), where an order parameter describes local water–oil concentration differences.[1] The free energy functional leads to the well-known Teubner–Strey expression for the scattering intensity of a bicontinuous microemulsion.[2] It allows the determination of the characteristic length scales of the microstructure, *i.e.* the periodicity d_{TS} and the correlation length ξ_{TS}.[3,4] The microemulsion structure is governed by the elastic constants, the bending rigidity κ and the saddle splay modulus $\bar{\kappa}$ of the surfactant membrane.[5] Structural investigation with scattering methods on a nanometer length scale and phase diagrams on macroscopic length scales reveals many aspects of the elastic properties of the membrane. The properties of microemulsions can be modified by addition of co-surfactants, *e.g.* diblock co-polymers, which increase the surfactant efficiency significantly and allow the emulsification of more water and oil with the same amount of surfactant.[6–8] The contrary effect is observed with the addition of homopolymers into the oil and water phase, and thus the efficiency of the surfactant is decreased.[3] Neutron spin echo spectroscopy accesses the membrane fluctuations on a local scale.[9,19] The elastic constants of droplet phases were investigated successfully by a combination of SANS and NSE experiments.[10] Polydispersity and droplet fluctuations are measured, which are both sums of κ and $\bar{\kappa}$ and allow the separation of both constants in droplet microemulsions. Recently, bicontinuous microemulsions with supercritical CO_2 as the oil phase, water and a fluorosurfactant have been investigated with scattering methods and phase diagram investigation.[11,12,21,22] This type of systems allows us to access different points in the phase diagram simply by changing the pressure of the system at a constant volume fraction of the surfactant and without additional co-surfactants. In this paper, we combine SANS, NSE and phase diagram measurements (as schematically depicted in Fig. 1). A combination of the different information from structural and dynamic investigation gives a detailed insight into the interplay between bending rigidity and saddle splay modulus. We will show that it is experimentally possible to separate different contributions from κ and $\bar{\kappa}_0$.

2 The different bending rigidities

2.1 Gaussian random field model

According to the Gaussian random field model (GRFM), the renormalized bending rigidity in units of k_BT is related to the structural length scale $d_{TS} = 2\pi/q_0$ and the correlation length ξ_{TS} as follows:[13]

$$q_0\xi_{TS} = \frac{64}{5\sqrt{3}}\kappa_{R,SANS} \quad (1)$$

[a]*Jülich Centre for Neutron Science JCNS, Forschungszentrum Jülich GmbH, Outstation at FRM II, Lichtenbergstr. 1, 85747 Garching, Germany. E-mail: o.holderer@fz-juelich.de; Fax: +49 89 289 10799; Tel: +49 89 289 10707*

[b]*Jülich Centre for Neutron Science JCNS (JCNS-1) & Institute of Complex Systems (ICS), Forschungszentrum Jülich GmbH, 52425 Jülich, Germany*

[c]*Department of Chemistry, University of Cologne, Luxemburger Str. 116, 50939 Cologne, Germany. E-mail: Thomas.Sottmann@uni-koeln.de; Fax: +49 221 470 5104; Tel: +49 221 470 6308*

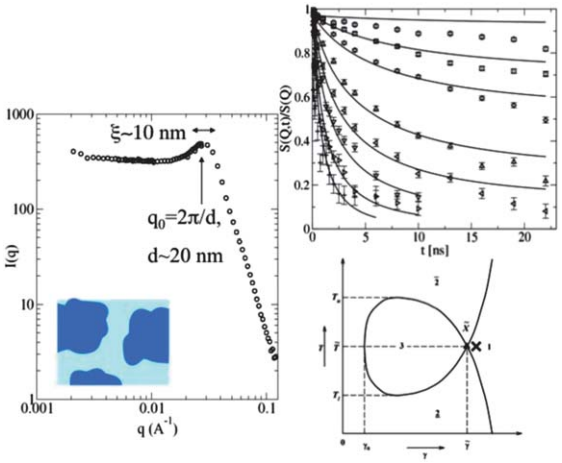

Fig. 1 SANS-curve (bulk contrast, recorded at X) gives structural parameters, the intermediate scattering function $S(q,t)$ measured by NSE represents local membrane fluctuations and allows the determination of the bending rigidity, and phase diagram data providing the saddle splay modulus with the position of the X point where the 1-phase region and the 3-phase region meet.

The index "SANS" is used since this bending rigidity is determined from small angle neutron scattering (SANS) experiments by fitting the Teubner–Strey formula[2] to the correlation peak in the scattering curve.The bending rigidity is renormalized due to the presence of fluctuations on length scales smaller than the experimental length scale d_{TS}.[14,15]The pure bending rigidity is linked to the renormalized one by:

$$\kappa_{R,SANS} = \kappa_{0,SANS} + \frac{1}{4\pi}\alpha \ln\left(\frac{2a}{d_{TS}}\right) \quad (2)$$

A similar equation holds for $\bar{\kappa}$ with a different prefactor $\bar{\alpha}$. The bending constants can also be determined by simulations with triangulated surfaces.[16] Recent simulations on triangulated surfaces[17] indicate that $\kappa_{R,SANS}$ determined in this way is not purely the bending rigidity κ, but a mixture of the bending rigidity and the saddle splay modulus $\bar{\kappa}$ rather than κ alone. The simplest ansatz, as used in ref. 17, assumes that the bending rigidity measured by SANS is a linear combination of the two with prefactors a_1 and a_2. One can then write for $\kappa_{0,SANS}$:

$$\kappa_{0,SANS} = \left(a_1\kappa_0 + a_2|\overline{\kappa_0}|\right) \quad (3)$$

Also the renormalization then needs to take into account this mixture with the same prefactors a_1 and a_2 and the known factors and from ref. 13.

The de-renormalization of the measured SANS bending rigidity then reads:

$$\kappa_{R,SANS} = \kappa_{0,SANS} + \frac{1}{4\pi}(\alpha a_1 + \bar{\alpha}a_2)\ln\left(\frac{2a}{d_{TS}}\right) \quad (4)$$

2.2 Phase diagrams

The saddle splay modulus can be obtained from the phase diagram, as has been described in ref. 13. At the X-point, *i.e.* the instability of the bicontinuous phase, the renormalized saddle splay modulus is zero,

$$\overline{\kappa_R} = 0 \quad \rightarrow \quad \overline{\kappa_0} = \frac{-\overline{\alpha}}{4\pi}\ln(\Psi) \quad (5)$$

where the logarithmic term in the renormalization factor contains the membrane volume fraction $\Psi = 2a/d_{TS}$.

2.3 NSE measurements

Neutron spin echo (NSE) spectroscopy, on the other hand, probes the membrane fluctuations on a local scale. From the intermediate scattering function one can deduce the bending rigidity by applying the Zilman–Granek formalism of a fluctuating membrane patch in a viscous medium.[18]

Since the NSE experiments probe the membrane fluctuations and on a local scale, one measures in this case the pure bending rigidity, without the renormalization term and without contributions from the saddle splay modulus:[19,20]

$$\kappa_{NSE} = \kappa_0 \quad (6)$$

2.4 SANS measurements: mixture of different modules

Using κ_0 from the NSE-experiment, $\kappa_{R,SANS}$ from SANS experiments and $\bar{\kappa}_0$ from the phase diagram, one can plug eqn (3), (5) and (6) into eqn (4) and then has

$$\begin{aligned}|\overline{\kappa_0}| &= \frac{1}{a_2}(\kappa_{0,SANS} - a_1\kappa_0) \\ &= \frac{1}{a_2}\left(\kappa_{R,SANS} - a_1\kappa_0 - \frac{1}{4\pi}(\alpha a_1 + \overline{\alpha a_2})\ln\left(\frac{2a}{d_{TS}}\right)\right)\end{aligned} \quad (7)$$

Eqn (7) contains the measured quantities $\kappa_{R,SANS}$, κ_0 (from NSE) on the right, the resulting saddle splay modulus can be set equal to the values of $\bar{\kappa}_0$ from the phase diagram. The factors a_1 and a_2 are then fitted as the only free parameters simultaneously for a set of microemulsions. These two factors describe the mixing of the bending rigidity and the saddle splay modulus in the renormalized bending rigidity determined by applying the GRFM to the SANS scattering curves.

2.5 Classical microemulsions

The determination of the factors a_1 and a_2 has been done with two types of microemulsions, "classical" oil–water–surfactant systems and supercritical CO_2-microemulsions. First, eqn (7) is applied to data for bicontinuous microemulsions containing $C_{10}E_4$, decane and water (with the volume fraction decane–water = 1) and homopolymers in the oil and water phase, namely PEP5 (polyethylene propylene, 5 kg mol^{-1}) and PEO5 (polyethylene oxide, 5 kg mol^{-1}) respectively. The homopolymer contents have been used to vary the bending rigidity as described in ref. 3 and 20. The phase diagram as well as SANS and NSE data have been presented in ref. 3 and 20. A set of two surfactant concentrations with two homopolymer concentrations has been taken for determining a_1 and a_2. The surfactant concentration has been 16% and 18.5%. Homopolymer concentrations of 0.25% and 0.5% for both surfactant concentrations have been included in the analysis. The values of $\bar{\kappa}_0$ from the phase diagram, κ_0 from NSE experiments and

$\kappa_{R,SANS}$ from the Teubner–Strey analysis of the SANS intensities are fed into eqn (7) for all available experimental points and the two parameters a_1 and a_2 are fitted simultaneously to all experimental data points (both surfactant concentrations, both homopolymer concentrations for each surfactant concentration). Table 1 compiles the relevant values.

The result is shown in Fig. 2. Both $\bar{\kappa}_0$ and κ_0 contribute to $\kappa_{R,SANS}$. The fitted factors $a_1 = 0.19$ and $a_2 = -0.84$ agree well with the simulation results of Gompper *et al.* ($a_1 = 0.148$ and $a_2 = -0.849$). The logarithmic term accounting for renormalization effects contains the membrane volume fraction $\Psi = 2a/d_{TS}$ with the membrane thickness a and the periodicity d_{TS}. For real microemulsions, it was found in ref. 3 that $d_{TS} = 37$ Å$/\Psi$. This value of Ψ has been first used for the fitting of the experimental data.

It turned out that the prefactor $(a_1\alpha + a_2\bar{\alpha})$ of the logarithmic term, which has to be close to 3 to be in agreement with the experimental data of ref. 13 is then much higher. The renormalization term in ref. 17 is written as $\ln(\delta S/V)$ with the cutoff length for short wavelength fluctuations δ which is set to be approximately the membrane thickness (to arrive at the volume fraction Ψ inside the ln). It has to be pointed out that this is not a strict choice. In the current evaluation, a three times higher cutoff, *i.e.* 3δ, is needed for the renormalization term (*i.e.* $\ln(3\Psi)$) to result in the prefactor $(a_1\alpha + a_2\bar{\alpha})$ of the logarithm term of 3.37, which is then consistent with the older data. Additionally, the error of the fit is minimized with a larger value of the cutoff than δ, the minimum lies, depending on the system, between 3δ and 6δ. The following data treatment uses throughout the cutoff value of 3δ.

2.6 Supercritical microemulsions

Recently, first NSE experiments on bicontinuous microemulsions containing supercritical CO_2 as the oil phase and a fluorosurfactant have allowed us to obtain the bare bending rigidity of these systems.[21,22] These systems allow us to access different points in the phase diagram simply by changing the applied pressure. Similar to the addition of homopolymers or diblock copolymers, the X-point shifts towards a lower surfactant concentration with increasing pressure. The set of obtained SANS (measured at D11 at the ILL[23]) and NSE data (from J-NSE at the FRM II research reactor[24]) allows us to then measure the bending rigidity of the same sample at different pressures, *i.e.* at different distances to the pressure dependent X-point.

First, the parameters a_1 and a_2 obtained above were simply applied to the data on supercritical microemulsions from ref. 22, see Table 2, without refitting. The result of this evaluation is shown in Fig. 3 with the fitted prefactors in the inset and the value of $\bar{\kappa}_0$ determined from SANS and NSE experiments according to eqn (7). The $\bar{\kappa}_0$-values from the phase diagram

Table 1 Data from NSE-, SANS-, and phase diagram measurements for bicontinuous microemulsions with homopolymers in the oil- and water-phase with homopolymer contents Φ_p, see ref. 20

Surf. conc. γ	Φ_p/%	κ_{NSE}/k_BT	$\kappa_{R,SANS}/k_BT$	$\bar{\kappa}_0/k_BT$	d_{TS}/nm
0.160	0.25	0.9	0.42	−0.52	24.9
0.160	0.5	0.8	0.40	−0.50	25.0
0.185	0.25	0.8	0.45	−0.52	20.6
0.185	0.5	0.7	0.42	−0.50	20.6

Table 2 Data from NSE-, SANS-, and phase diagram measurements for bicontinuous supercritical CO_2-microemulsions at pressure P, see ref. 22

Surf. conc. γ	P/bar	κ_{NSE}/k_BT	$\kappa_{R,SANS}/k_BT$	$\bar{\kappa}_0/k_BT$	d_{TS}/nm
0.262	200	0.57	0.35	−0.49	27.9
0.262	250	0.74	0.38	−0.55	29.0
0.262	300	0.82	0.39	−0.58	29.2
0.350	160	0.53	0.45	−0.40	17.6
0.350	200	0.63	0.47	−0.49	18.3
0.350	250	0.70	0.49	−0.55	18.4
0.350	300	0.68	0.48	−0.58	18.8

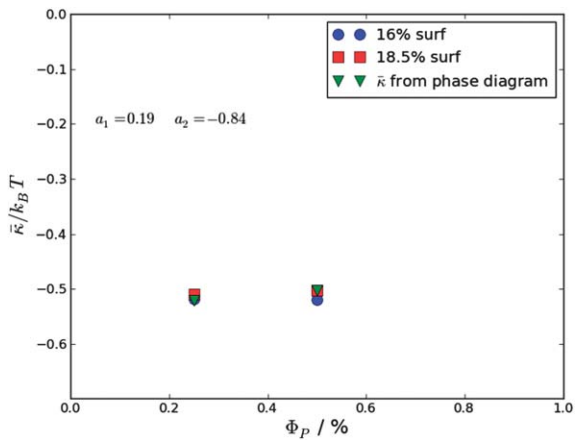

Fig. 2 Homopolymer microemulsions with two different surfactant concentrations: fitting the calculated values of the saddle splay modulus from NSE and SANS experiments according to eqn (7) to the saddle splay modulus determined from the phase diagram yielding the values of a_1 and a_2.

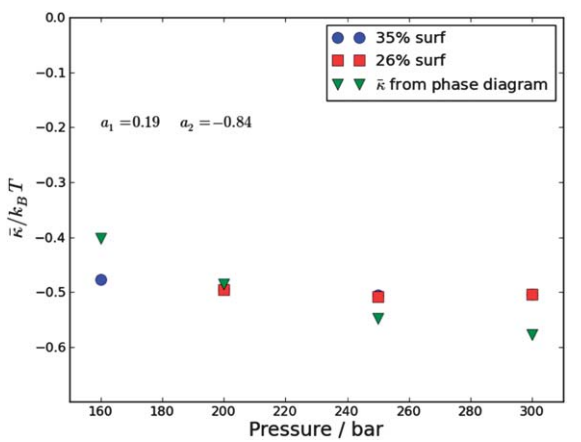

Fig. 3 Supercritical CO_2-microemulsions with two different surfactant concentrations: calculated $\bar{\kappa}$ with parameters a_1 and a_2 taken from the fit with the homopolymer sample, compared with the saddle splay modulus from phase diagram measurements.

show a pressure dependence, while the ones determined by NSE and SANS are rather constant with pressure. One has to point out that the neutron scattering experiments performed to determine $\bar{\kappa}_0$ are done at one surfactant concentration and different pressures. Starting close to the X-point at low pressures, the X-point moves to lower surfactant (membrane) concentrations increasing the pressure. However the $\bar{\kappa}_0$ determination from the phase diagram is always done at the X-point, *i.e.* at different membrane concentrations. The results indicate that the saddle splay modulus is constant with pressure at one surfactant concentration, *i.e.* at different points in the fish tail of the phase diagram, but varies slightly with varying surfactant concentration.

In a second step, the prefactors a_1 and a_2 have been fitted simultaneously for the lowest pressures for each surfactant concentration, *i.e.* for the point closest to the X-point (that is 160 bar for 35% surfactant concentration and 200 bar for 26% surfactant concentration). The reason of choosing only the lowest pressure in this fitting procedure is that only at the X point the determination of $\bar{\kappa}_0$ from the phase diagrams is possible. One arrives at the values $a_1 = 0.15$ and $a_2 = -1.02$ and the resulting saddle splay moduli as shown in Fig. 4. Both cases, the fixed set of parameters a_1 and a_2 from the "classical" microemulsions and the set fitted to the data of the supercritical microemulsion, are very close to the simulated parameters a_1 and a_2.

2.7 An alternative route

While using NSE as the method to determine the bare bending rigidity, an alternative route may rely on the phase diagram and SANS data only, even though the experimental uncertainties stay a little larger. All experimental database on the experiments[4] involve homopolymers and diblock copolymers simultaneously as additives. We change the fundamental SANS equation (eqn (1)) to the following:

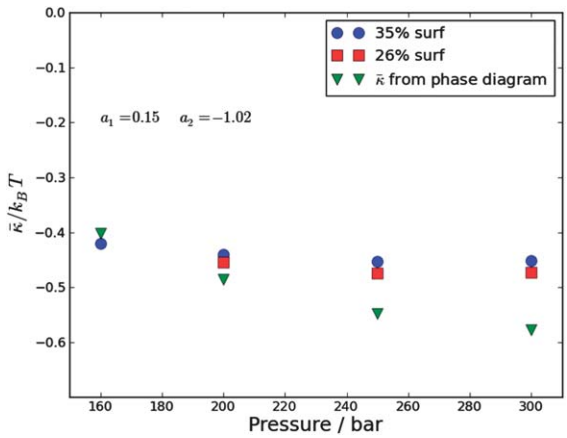

Fig. 4 Supercritical CO_2-microemulsions with two different surfactant concentrations as in Fig. 3: a_1 and a_2 are now re-determined by fits of the saddle splay modulus calculated with eqn (7) to the one from phase diagram measurements at the lowest pressure for each surfactant concentration (160 bar for 35% surfactant conc. and 200 bar for 26% surfactant conc.). The values for higher pressures for each surfactant concentration are then calculated with these new parameters.

$$\frac{S}{V}\xi_{TS} = A_{SANS}\kappa_{R,SANS} \tag{8}$$

The surface per volume ratio of the surfactant film is simply given by $S/V = \Psi/a$ with a being the film thickness ($a = 12$ Å for $C_{10}E_4$ from ref. 4). The amplitude is according to the GRFM theory[6] $A_{SANS} = 128/15\pi$. Also the simulations from ref. 17 (Fig. 7) lead to a very similar value of $A_{SANS} \approx 3$. The influence of the added diblock copolymers and homopolymers on the elastic constants has been described in theory.[25,26] For the elastic moduli we get the following from these theories:[4]

$$\kappa_R = \kappa_0 + \frac{\alpha}{4\pi}\left(\ln\Psi - \beta\frac{\phi_P}{V_P}\left(R_{hW}{}^3 + R_{hO}{}^3\right) + \Xi\sigma\left(R_{dW}{}^2 + R_{dO}{}^2\right)\right) \tag{9}$$

$$\bar{\kappa}_R = \bar{\kappa}_0 + \frac{\bar{\alpha}}{4\pi}\left(\ln\Psi - \bar{\beta}\frac{\phi_P}{V_P}\left(R_{hW}{}^3 + R_{hO}{}^3\right) + \bar{\Xi}\sigma\left(R_{dW}{}^2 + R_{dO}{}^2\right)\right) \tag{10}$$

In theory, the coefficients α, β, and Ξ (and corresponding ones for the saddle splay modulus) are known. For the current section, it is assumed that $\alpha = 3$ and $\bar{\alpha} = -10/3$ are known. Furthermore, it is assumed that the ratios $\beta/\bar{\beta} = 1.253$ and $\Xi/\bar{\Xi} = 1.428$ are known from theory.[6] κ_0 and $\bar{\kappa}_0$ are bare parameters at the extrapolated surfactant concentration $\Psi = 1$ (limit of no fluctuations). Then, the SANS measurements would find a mixed state from both κ and $\bar{\kappa}$, according to:

$$\kappa_{R,SANS} = b \times \kappa_R - (1 - b) \times \bar{\kappa}_R \tag{11}$$

with the renormalized moduli in analogy to eqn (3). Simultaneously, the fish tail points of the different samples are described by setting the saddle splay modulus to be constant:[27]

$$\bar{\kappa}_{R,SANS}(\Psi) = \bar{\kappa}_{phaseb.} = 0.28 \tag{12}$$

The constant value $\bar{\kappa}_{phaseb.}$ is neglected in many studies. We finally chose this value to obtain similar values for the constant terms $\kappa_0 \approx -\bar{\kappa}_0$, but there is no experimental evidence for this

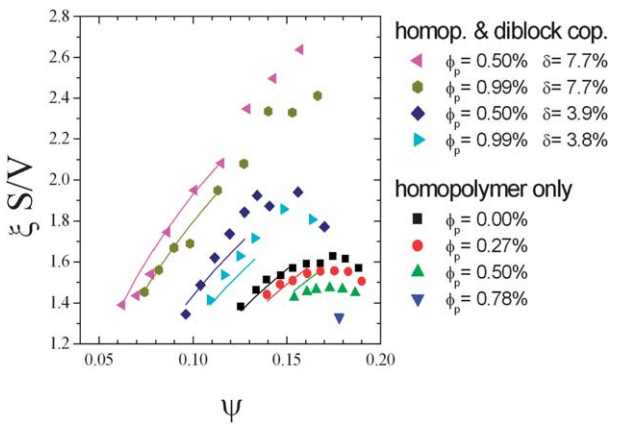

Fig. 5 Evaluation of the SANS data from eqn (8)–(11), simultaneously with the phase boundary data (Fig. 6). Data points arise from single measurements. For the fitting lines, only points close to the fish tail point were taken into account. The common range indicates which points were selected.

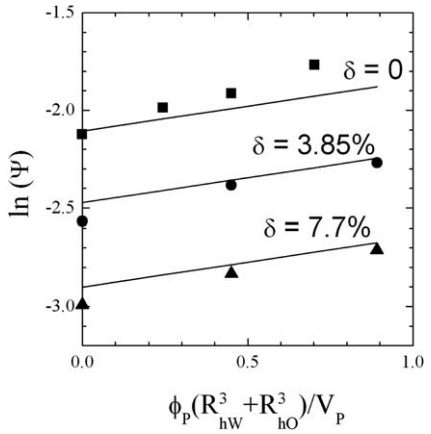

Fig. 6 Phase boundary data (fish tail points) as a function of the scaled homopolymer amount. The solid lines arise from the simultaneous fitting.

Table 3 Coefficients of the alternative route (note the ratios of the coefficients are set as well). All bending rigidities are given in units of k_BT

Parameters	Theory for κ	Theory for $\bar{\kappa}$	Experiment for κ	Experiment for $\bar{\kappa}$
α	3	−10/3	Set	Set
β	0.0996	0.0795	0.319	0.254
Ξ	0.897	0.628	1.84	1.29
κ_0	—	—	−0.930	−0.839
A_{SANS}	2.716		4.36	
b	(1.00)		0.166	

exact result. Now all data from homopolymer microemulsions and diblock-copolymer microemulsions can be fitted simultaneously (Fig. 5).

The final result including the phase boundary information is presented in Table 3. The values for β, $\bar{\beta}$ and $\bar{\Xi}$ agree roughly with the experimental values determined in ref. 3, while Ξ is larger (experimental $\Xi \approx 0.4$ in ref. 3). The discrepancies appear due to the simultaneous fitting and fixing the ratios of the coefficients.

The final value b has to be compared with the previous $a_1/(a_1 - a_2)$ of the NSE evaluations that take values in the range of 0.13 to 0.18 and with the theoretical[13] value of 0.15. With taking the errors into account (we have *ca.* 30% error for b) all values are basically identical.

3 Conclusions

This set of experiments is, to our knowledge, the first experimental determination of the different moduli determining the elastic properties of surfactant membranes, $\bar{\kappa}_0$ and κ_0, and the influence of the two in the measurement of $\kappa_{R,SANS}$. The basic assumption (eqn (3)) that $\kappa_{R,SANS}$ is a linear combination of $\bar{\kappa}_0$ and κ_0 is inferred from ref. 17 as the simplest ansatz consistent with the simulations. The combination of phase diagram measurements together with SANS- and NSE-experiments provided the necessary information to separate the different contributions and to determine the parameters a_1 and a_2 experimentally. The short wavelength cutoff for the renormalization term, δ, has been found to be approximately 3 times the membrane thickness in order to minimize the fitting error and to give prefactors of the log-term consistent with the experiments in ref. 13. The statistical variation of the fit parameters κ in the different experiments is rather small (∼1% for SANS and ∼5% NSE experiments), however, the combination together with the uncertainities in the models (*e.g.* the cutoff length δ) leads to an overall precision of this approach of 10–20% in our opinion. Different kinds of microemulsions, namely classical bicontinuous microemulsions containing $C_{10}E_4$, D-decane and D_2O and the homopolymers PEP and PEO in the oil and water phase respectively, have been analyzed as well as supercritical microemulsions with CO_2 as the oil phase. Both types of microemulsions showed the same behavior with almost the same numerical values for a_1 and a_2. The experimental result that both $\bar{\kappa}_0$ and κ_0 contribute to $\kappa_{R,SANS}$ is a rather general result valid for different types of microemulsions and they confirm the mixing parameters a_1 and a_2 from recent simulations on triangulated membrane surfaces.[17] Two different paths, a combination of SANS, NSE and phase diagram measurements on the one hand and a simultaneous fit of SANS and phase diagram data with different additives on the other hand, result in the same mixing parameters within the accuracy of the experiments. Supercritical microemulsions offer in this context a new possibility to vary the point of observation in the phase diagram in static and dynamic scattering experiments by changing the pressure with otherwise unchanged molar fractions of the components and without additional co-surfactants.

Acknowledgements

We wish to thank G. Gompper, T. Auth and M. Peltomäki for fruitful discussion. We also wish to thank the EU-network of excellence SoftComp for financial support.

Notes and references

1 G. Gompper and M. Schick, in *Phase Transitions and Critical Phenomena*, ed. C. Domb and J. Lebowitz, Academic Press, London, 1994.
2 M. Teubner and R. Strey, *J. Chem. Phys.*, 1987, **87**, 3195–3200.
3 T. Sottmann, R. Strey and S. H. Chen, *J. Chem. Phys.*, 1997, **106**(15), 6483.
4 D. Byelov, H. Frielinghaus, O. Holderer, J. Allgaier and D. Richter, *Langmuir*, 2004, **20**, 10433–10443.
5 W. Helfrich, *Z. Naturforsch.*, 1973, **28**, 693.
6 H. Endo, J. Allgaier, G. Gompper, B. Jakobs, M. Monkenbusch, D. Richter, T. Sottmann and R. Strey, *Phys. Rev. Lett.*, 2000, **85**, 102–105.
7 H. Endo, M. Mihailescu, M. Monkenbusch, J. Allgaier, G. Gompper, D. Richter, B. Jakobs, T. Sottmann, R. Strey and I. Grillo, *J. Chem. Phys.*, 2001, **115**, 580–600.
8 B. Jakobs, T. Sottmann, R. Strey, J. Allgaier, L. Willner and D. Richter, *Langmuir*, 1999, **15**, 6707–6711.
9 B. Farago, D. Richter, J. S. Huang, S. A. Safran and S. T. Milner, *Phys. Rev. Lett.*, 1990, **65**, 3348.

10 T. Hellweg, M. Gradzielski, B. Farago and D. Langevin, *Colloids Surf., A*, 2001, **183–185**, 159–169.
11 M. Klostermann, L. G. A. Kramer, T. Sottmann and R. Strey, *Phys. Chem. Chem. Phys.*, 2011, **12**, 6247–6252.
12 M. Schwan, L. Kramer, T. Sottmann and R. Strey, *Phys. Chem. Chem. Phys.*, 2010, **12**, 6247–6252.
13 G. Gompper, H. Endo, M. Mihailescu, J. Allgaier, M. Monkenbusch, D. Richter, B. Jakobs, T. Sottmann and R. Strey, *Europhys. Lett.*, 2001, **56**, 683–689.
14 L. Peliti and S. Leibler, *Phys. Rev. Lett.*, 1985, **54**, 1690.
15 D. Roux, F. Nallet, C. Coulon and M. E. Cates, *J. Phys. II*, 1996, **6**, 91.
16 G. Gompper and D. Kroll, *Phys. Rev. Lett.*, 1998, **81**, 2284–2287.
17 M. Peltomäki, G. Gompper and D. Kroll, *J. Chem. Phys.*, 2012, **136**, 134708.
18 A. G. Zilman and R. Granek, *Phys. Rev. Lett.*, 1996, **77**, 4788–4791.
19 M. Mihailescu, M. Monkenbusch, H. Endo, J. Allgaier, G. Gompper, J. Stellbrink, D. Richter, B. Jakobs, T. Sottmann and B. Farago, *J. Chem. Phys.*, 2001, **115**, 9563–9577.
20 O. Holderer, H. Frielinghaus, D. Byelov, M. Monkenbusch, J. Allgaier and D. Richter, *J. Chem. Phys.*, 2005, **122**, 094908.
21 O. Holderer, M. Klostermann, M. Monkenbusch, R. Schweins, P. Lindner, R. Strey, D. Richter and T. Sottmann, *Phys. Chem. Chem. Phys.*, 2011, **13**, 3022–3025.
22 M. Klostermann, R. Strey, T. Sottmann, R. Schweins, P. Lindner, O. Holderer, M. Monkenbusch and D. Richter, *Soft Matter*, 2012, **8**, 797–807.
23 P. Linder and R. Schweins, *Neutron News*, 2010, **21**(2), 15–18.
24 O. Holderer, M. Monkenbusch, G. Borchert, C. Breunig and K. Zeitelhack, *Nuclear Instruments & Methods in Physics Research Section a-Accelerators Spectrometers Detectors and Associated Equipment*, 2008, vol. 586, pp. 90–94.
25 C. Hiergeist and R. Lipowsky, *J. Phys. II*, 1996, **6**, 1465.
26 A. Hanke, E. Eisenriegler and S. Dietrich, *Phys. Rev. E: Stat. Phys., Plasmas, Fluids, Relat. Interdiscip. Top.*, 1999, **59**, 6853.
27 D. C. Morse, *Phys. Rev. E: Stat. Phys., Plasmas, Fluids, Relat. Interdiscip. Top.*, 1994, **50**, R2423.